

# Drag of Rectangular Cavities in Supersonic and Transonic Flow Including the Effects of Cavity Resonance

O. WAYNE MCGREGOR\*

*Fort Worth Division of General Dynamics, Fort Worth, Tex.*

AND

ROBERT A. WHITE†

*University of Illinois at Urbana-Champaign, Urbana, Ill.*

The drag of relatively short rectangular cavities (length-to-depth ratios of 0.50-3.0) with turbulent shear layers has been measured at transonic and supersonic Mach numbers (0.3-3.0). Of particular importance is the effect of pressure oscillations within the cavity (commonly referred to as cavity resonance) which is shown to increase the drag as much as 250%. Cavity resonance is found to occur over the entire Mach number range investigated and other work has shown it to occur at both lower and higher Mach numbers. The frequency of the pressure oscillations is best predicted by the vortex-wave interaction model presented by Rossiter. The effects of external reinforcement of resonance by reflection of radiated pressure waves are examined both experimentally and analytically. Existing methods for predicting cavity drag are inadequate to cope with this phenomena. A new model for predicting the lower bound of cavity drag (nonresonating cavity) is presented and agrees well with experimental data. Analytical considerations are utilized to indicate the qualitative effect of resonance on cavity drag.

## Nomenclature

$b$	= notch length
$C_D$	= drag coefficient, $D/[\frac{1}{2}(\gamma M_\infty^2 P_\infty b)]$
$C_p$	= pressure coefficient, $\Delta P/[\frac{1}{2}(\gamma M_\infty^2 P_\infty)]$
$c$	= acoustic velocity
$D$	= drag per unit width
$d$	= notch depth
$f$	= frequency
$h$	= wind-tunnel height
$M$	= Mach number, $u/c$
$P$	= pressure
$\Delta P$	= peak-to-peak pressure amplitude
$St$	= Strouhal number, $fb/u_\infty$
$u$	= flow velocity
$W$	= interaction parameter, see Eq. (A1)
$w$	= shear layer deflection
$x$	= horizontal position
$y$	= vertical position
$\gamma$	= ratio of specific heats
$\delta$	= boundary-layer thickness
$\eta$	= dimensionless shear layer deflection, $w/b$
$\rho$	= fluid density
$\sigma$	= turbulent jet spreading parameter, $12 + 2.758 M_\infty$
$\phi$	= dimensionless velocity, $u/u_\infty$

## Subscripts

$\infty$	= freestream
$s$	= separating streamline
$v$	= vortex
$u$	= upper shear layer boundary
$L$	= lower shear layer boundary
$i$	= inward shear layer deflection
$o$	= outward shear layer deflection

Received October 24, 1969; revision received April 1, 1970. This work was partially supported by the National Science Foundation under Grant NSF GK-2053. The authors also wish to acknowledge the cooperation of the Aeronautical Research Institute of Sweden which made possible a number of the experiments.

\* Graduate Research Assistant, now Senior Aerodynamics Engineer. Associate Member AIAA.

† Associate Professor of Mechanical Engineering.

## 1. Introduction

THE existence of notches or grooves in both external and internal aerodynamic configurations is a fact. These may exist as a design goal, as in aircraft landing gear wells or in bomb bays, or as an unavoidable result as with partially deflected flaps or in pipe fittings. It has been suggested<sup>1</sup> that because of their heat transfer and drag characteristics cavities may be a desirable part of design features of aerospace vehicles. Regardless of the reason for their existence, it is necessary for the designer to be knowledgeable of the effects on the configuration of which they are a part.

Although it has been known for some time that cavities often emit strong acoustical radiation<sup>2-4</sup> in conjunction with internal pressure oscillations, no drag data concerning effects of this phenomenon have been available. In addition, all but one of the analytical models for treating such flows have assumed nonoscillating flow<sup>5-7</sup> and, consequently, are inadequate for such cases. Moreover, only one model<sup>8</sup> attempts to handle both high and low Mach numbers. Charwat et al.,<sup>8</sup> suggested a model for heat transfer within cavities when pressure oscillations occur. This model, which is physically perceptive, assumes equal shear layer displacement into and out of the cavity at the reattachment point, violating continuity of mass within the cavity.

This paper considers the drag of rectangular cutouts or notches spanned by turbulent shear layers and how it is affected by the important variables, including cavity resonance. Experimental data over a range or Mach number, cavity size, and Reynolds number are presented. Both internal and external aerodynamic configurations are considered. Analytical considerations are presented which lend insight into the over-all cavity problem. These considerations are applicable at both high and low Mach numbers.

## 2. Experimental Investigation

### 2.1 Experimental Facilities

Because of the complex nature of the flow within cavities, particularly during resonance, the results of the experimental

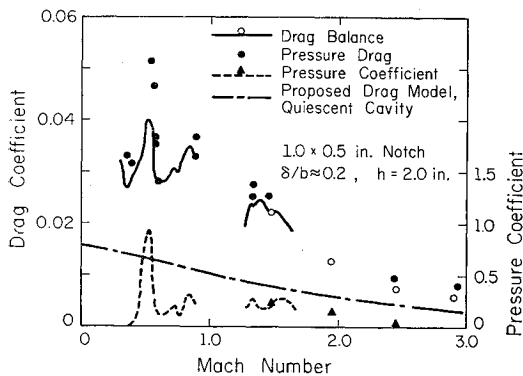


Fig. 1 Drag and pressure oscillation amplitude data for a typical rectangular notch.

investigation are presented first. This leads to a better understanding of the analytical considerations of Sec. 3.

The experiments were performed in two separate facilities. The majority of the work was carried out in the wind tunnels at the University of Illinois at Urbana-Champaign.<sup>‡</sup> These wind tunnels are of the blowdown type and have  $2 \times 4$ -in. (half nozzle) test sections in the supersonic range. For the transonic experiments, a slotted wall tunnel ( $4 \times 4$ -in. test section) and a solid wall tunnel ( $2 \times 4$ -in. test section) were used. The size of these facilities made it difficult to perform a number of desired experiments; consequently, these were carried out in the  $18 \times 19$ -in. S5 transonic wind tunnel of the Aeronautical Research Institute of Sweden.<sup>†</sup>

## 2.2 Experimental Determination of Cavity Drag

The drag of the cavities was measured using a direct measuring drag balance for finite aerodynamic elements developed by Howell.<sup>10</sup> The drag of a smooth flat plate was measured during each series of tests and was within 10% of the data presented by Spalding and Chi.<sup>11</sup> A further check on the balance accuracy was made by instrumenting a cavity with pressure taps on both the upstream and downstream faces. The drag was obtained by integration of pressure forces over the faces. As shown in Fig. 1, agreement between these data and those obtained by the drag balance is good.

Tests which simultaneously measured the notch drag and the amplitude of the pressure oscillations on the notch floor were made over the Mach number range 0.3–3.0 for various notch sizes. Results for a typical notch are shown in Fig. 1. The direct correspondence between drag peaks and pressure peaks demonstrates that cavity drag is increased by resonance. The magnitude and occurrence of the peaks are partially caused by the wind-tunnel interference discussed in the Appendix. A comparison of drag for three notches of the

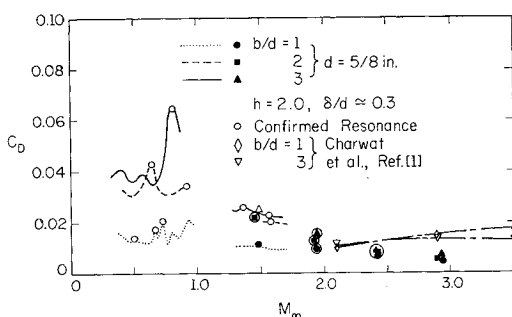


Fig. 2 Drag variation measured for three notches of different lengths.

<sup>‡</sup> Complete descriptions of these facilities are given in Refs. 8 and 9.

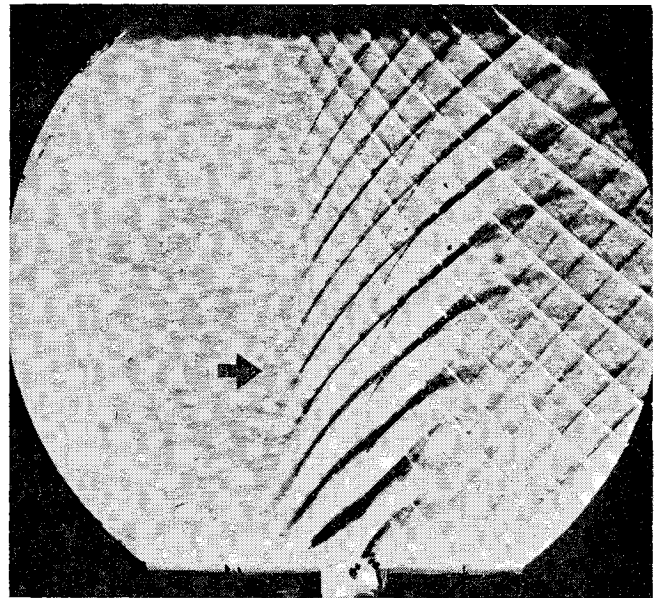


Fig. 3 Schlieren photograph of  $50 \times 40$  mm notch in transonic flow ( $M_\infty = 0.902$ ).

same depth and with the same approaching boundary-layer thickness is made in Fig. 2. The indicated trend of decreasing drag with increasing  $\delta/b$  was found to be true for all notches tested and agrees with the theoretical model of Sec. 3 (see Fig. 9).

## 2.3 Experimental Investigation of Cavity Flow

The problem initially conceived of constructing a cavity that exhibited resonance turned out to be redundant. Indeed, the problem has been to build a cavity that does not resonate. It was found that all of the cavities constructed resonated at one or more Mach numbers. Figure 3 is a schlieren photograph showing the typical response of a cavity in subsonic flow.

The pressure response of cavities during a continuous change of Mach number ( $M_\infty = 0.4$ – $1.5$ ) was investigated utilizing high-frequency piezoelectric pressure transducers and a multiple-channel recording system. Figure 4 shows the variation of the amplitude of the pressure oscillations at the base of the upstream notch wall for two cavity sizes. A distinct pattern of strong and weak pressure oscillations is particularly noticeable in the subsonic regime. The “peaks” have been found to correspond to an almost sinusoidal pressure oscillation, while the “valleys” correspond to a transient change between the frequency of the preceding peak and twice that frequency. Typical conditions are shown by the insets in Fig. 4.

An earlier water table investigation<sup>12</sup> suggested that the internal cavity flow was dominated by a transverse wave action. This had been postulated by Rossiter,<sup>4</sup> who also found the existence of streamwise moving vortices within the shear layer. A series of high-speed schlieren photographs (approx. 9000 frames/sec) was taken to determine the flow pattern within the cavity. These photographs (a typical sequence is shown in Fig. 5) confirm the existence of both a transverse wave (not shown here) and a series of vortices emanating from the separation point and moving downstream along the shear layer.

As indicated in Fig. 3, the shear layer spanning the cavity is deflected when the cavity resonates. The amplitude of this deflection was measured by monitoring the shear layer recompression pressure at the downstream corner of the cavity. Shear layer deflections based on the velocity profile presented in Sec. 3 are shown in Fig. 6. At  $M_\infty = 0.52$  the resonance intensity was such that the lower pressure level dropped below

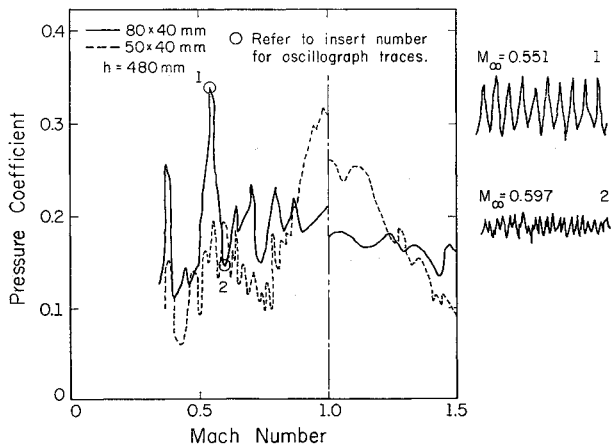


Fig. 4 Amplitude of pressure oscillations and typical pressure histories within two rectangular notches ( $\delta/d = 0.5$ ).

the freestream pressure, indicating flow out of the notch along the rear wall.

#### 2.4 Pressure Oscillation Frequency

Of the frequency prediction models currently available (Refs. 4, 12-14), the vortex-wave interaction model proposed by Brown<sup>15</sup> and Rossiter<sup>4</sup> provides the best prediction. In this model, a vortex forms in the shear layer near the upstream corner of the cavity and is transported downstream with the average velocity  $\phi_v$ . When the vortex impacts the downstream cavity wall, a pressure wave is produced which radiates from the wall with velocity  $c$ . It is assumed that there is a time lapse of  $\beta/f$  between the time the vortex arrives and the time when the wave is radiated. The arrival of this pressure wave at the origin of the shear layer provides the needed perturbation to form a new vortex in the shear layer. Both the pressure wave and the vortex postulated here have been observed experimentally during this investigation. Requiring the frequency of the vortex and pressure wave

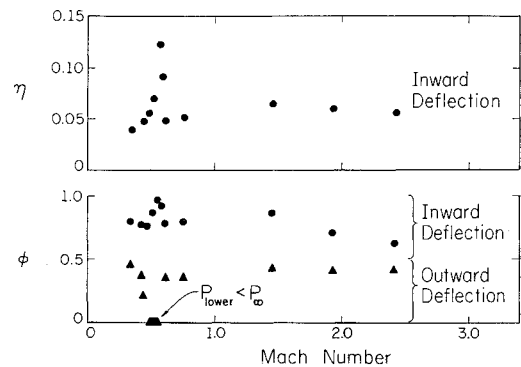


Fig. 6 Shear layer deflection in  $1.5 \times 0.5$  in. notch based on assumed velocity profile [Eq. (3)].

generation to be equal and applying geometric considerations yields

$$St = (m - \beta) / [M_\infty(c_\infty/c) + 1/\phi_v] \quad (1)$$

where  $m$  is the total number of vortices and pressure waves participating.

As shown in Fig. 7, Eq. (1) predicts the dimensionless frequency very well when it is assumed that the pressure wave travels at the freestream sonic velocity, when  $\beta = 0.25$  and when the vortex transport velocity is defined by  $\phi_v$ , the velocity along the jet-streamline.<sup>16</sup> As illustrated by the dashed line, the frequency for a given cavity increases in distinct steps with increasing Mach number.<sup>12</sup> Since no change in frequency is noted as the Mach number exceeds 1.10 (the Mach number above which reflected waves no longer intercept the cavity), the resonant frequency must be independent of opposite wall effects.

### 3. Proposed Model for the Drag of a Resonant Cavity

When the cavity resonates, the shear layer is deflected and pumps mass having a high level of momentum into the notch.<sup>8</sup> The mass is slowed down by various dissipative processes within the cavity, and, by its presence, causes the cavity pressure to exceed the freestream pressure. The shear layer is then deflected out of the notch by the excess pressure, and mass is pumped out of the cavity with a lower level of momentum. This oscillatory process is continued with the net effect that the freestream loses some momentum with the passage of each cycle. The rate at which this momentum is lost is the drag contribution of pressure oscillations. Omitting the effects of shear layer curvature, the total drag is the drag of a quiescent cavity plus the resonant contribution.

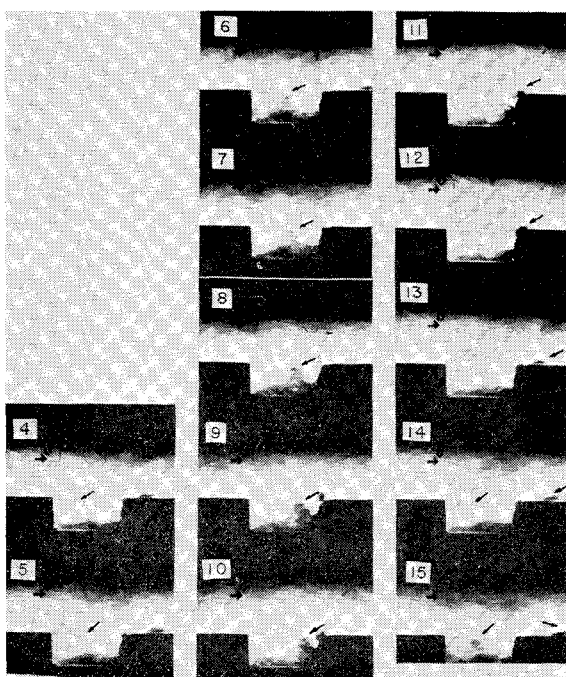


Fig. 5 Sequential schlieren photographs of  $80 \times 40$  mm notch showing transverse vortex formation ( $M_\infty = 0.555$ ).

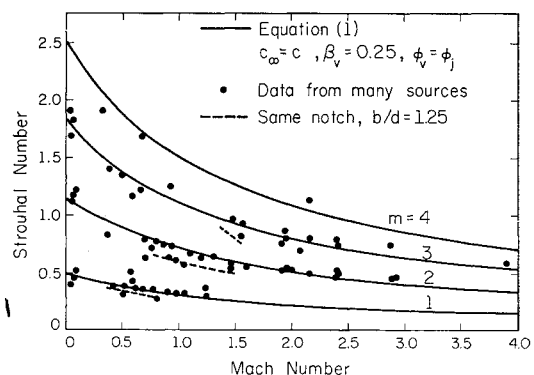


Fig. 7 Frequency of pressure oscillations measured in notches compared to the predicted frequency.

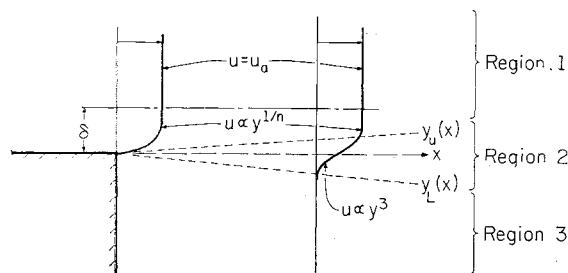


Fig. 8 Flow configuration for theoretical drag model.

### 3.1 Drag of a Quiescent Cavity

No satisfactory model presently exists for the prediction of the drag of a nonresonant cavity. The analysis by Haugen and Dhanak<sup>6</sup> is suitable, but is valid only for incompressible flows. The analysis by Golik<sup>5</sup> is also applicable, but does not accurately include effects of the approaching boundary layer. The drag model proposed here, which is similar to that of Haugen and Dhanak, includes both compressibility and boundary-layer effects.

The flowfield in the neighborhood of the cavity opening is divided into three distinct, interacting regions as illustrated in Fig. 8. The effects of the secondary flow within the cavity (region 3) are being neglected here; however, they can be included<sup>17</sup> if sufficient information is available about the secondary flow. Following the example of Haugen and Dhanak,<sup>6</sup> the velocity profile of the boundary layer is assumed to remain unchanged in region 1. The velocity profile within the shear layer (region 2) is approximated by the cubic polynomial

$$u = a_0 + a_1 y + a_2 y^2 + a_3 y^3 \quad (2)$$

Requiring both the velocity and the velocity gradient to match external conditions at the boundaries of the shear layer defines the coefficients to be

$$\begin{aligned} a_3 &= [2u_u + (y_L - y_u)u_u'] / (y_L - y_u)^3, \\ a_2 &= \frac{1}{2} [-u_u' - 3(y_L^2 - y_u^2)a_3] / (y_L - y_u) \\ a_1 &= u_u' - (2y_u a_2 + 3y_u^2 a_3), \\ a_0 &= u_u - (y_u a_1 + y_u^2 a_2 + y_u^3 a_3) \end{aligned}$$

where prime denotes differentiation with respect to  $y$  and

$$u_u = u_\infty (y_u / \delta)^{1/n}$$

The upper and lower boundaries are defined by (based on data from Refs. 18 and 19)

$$y_u = 1.2x/\sigma, \quad y_L = 1.5x/\sigma$$

where  $\sigma$  is the similarity parameter defining the spreading

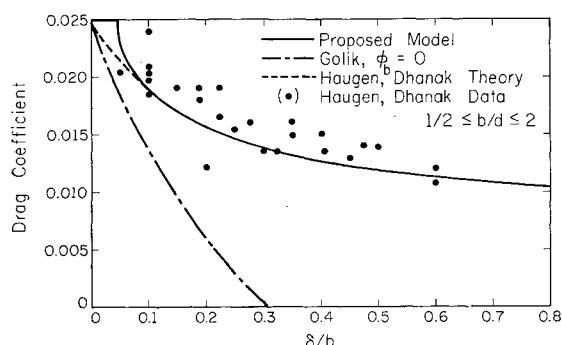


Fig. 9 Theoretical cavity drag as a function of thickness of approaching boundary layer ( $M_\infty = 0$ ).

rate of turbulent free jets.<sup>5</sup> Shear stress along the streamline separating the free stream from the separated wake is

$$\tau_s = \rho_s \epsilon_t \left. \frac{\partial u}{\partial y} \right|_{y=0}$$

where  $\epsilon_t$  is the momentum eddy diffusivity. For incompressible flows  $\epsilon_t$  is<sup>18</sup> given by

$$\epsilon_t = \frac{1}{2} c^3 x^2 \left. \frac{\partial u}{\partial y} \right|_{y=0}$$

where  $c$  is the similarity parameter governing the turbulent jet spreading rate. This relation may be extended to compressible flows by replacing  $c$  by  $1/\sigma$ ; thus,

$$\epsilon_t = \frac{1}{2} \frac{x^2}{\sigma^3} \left. \frac{\partial u}{\partial y} \right|_{y=0}$$

Using this relation and letting the shear stress at the midpoint of the notch approximate the average shear stress, the drag coefficient of a quiescent cavity is

$$C_D = (1/4\sigma^3)(\rho_o/\rho_\infty)(a_1 b/u_\infty)^2 \quad (3)$$

A comparison between the drag predicted by this model and that predicted by the models by Golik<sup>5</sup> and Haugen and Dhanak<sup>6</sup> for incompressible flow is shown by Fig. 9. Note that the Golik prediction is not satisfactory for large boundary layers. The agreement between the proposed model and that of Haugen and Dhanak is excellent for  $\delta/b > 0.05$  and at  $\delta/b = 0$ . Figure 10 illustrates the manner in which predicted drag changes with Mach number for various boundary-layer thicknesses. The case with  $\delta/b = 0$  is seen to agree with the drag predicted by Golik's model. These two comparisons demonstrate the ability of this relatively simple model to predict effects of both compressibility and boundary-layer thickness on the drag of rectangular notches. Since resonance has been shown to increase the cavity drag, the drag for a quiescent cavity [Eq. (3)] defines the lower limit of the drag of a rectangular notch. This is demonstrated in Fig. 1, where the predicted drag is less than the measured drag. This was true for all configurations tested. The difference is seen to be substantial in the vicinity of the peaks (as much as 250%).

### 3.2 Drag Contribution by Resonance Effects

The drag contribution by resonance effects may be estimated by computing the momentum flux into and out of the notch as a result of the deflection of the shear layer. In this analysis the shear layer will be assumed to alternate between the innermost and outermost positions. This will yield a larger drag than the more accurate assumption of a sinusoidally varying shear layer deflection, but will simplify the analysis considerably.

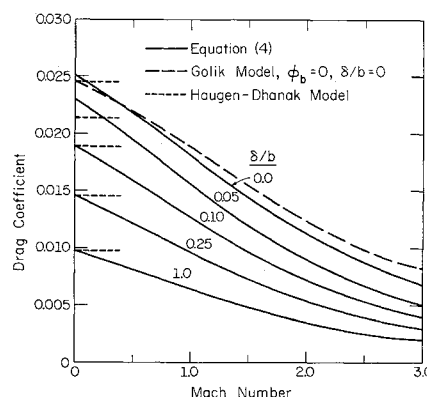


Fig. 10 Theoretical cavity drag as a function of freestream Mach number.

For the case of periodic deflections the net mass added to the notch during the first half-cycle must equal the net mass removed during the second half-cycle. This requirement fixes the relationship between the inward deflection and the outward deflection to be

$$\int_{-w_o}^0 \rho u dy = \int_0^{w_i} \rho u dy \quad (4)$$

where  $\rho u$  is given by the shear layer velocity profile [Eq. (2)] at  $x = b$ . In general, the mass flux ( $\rho u$ ) below the separating streamline ( $y = 0$ ) is less than the mass flux above the streamline; consequently, the outward deflection is greater than the inward deflection. Charwat's model<sup>3</sup> violates conservation of mass within the cavity by assuming equal deflections of the shear layer.

The drag induced by these deflections is

$$C_D = \int_0^{\eta_i} \left( \frac{\rho}{\rho_\infty} \right) \varphi^2 d\eta - \int_{-\eta_o}^0 \left( \frac{\rho}{\rho_\infty} \right) \varphi^2 d\eta \quad (5)$$

where  $\eta = w/b$  and  $x = b$ . Equation (5) defines an upper limit on the contribution of resonance to the drag of a cavity in terms of  $\eta_i$  or  $\eta_o$ . At present no theory is available for the prediction of either  $\eta_i$  or  $\eta_o$ . Some indication of the size of  $\eta_i$  is available from the data in Fig. 6, where the magnitude of the inward deflection  $w_i$  is indicated for the 1-in.  $\times$   $\frac{1}{2}$ -in. cavity. Figure 11 compares the drag computed using Eqs. (5) and (3) for various values of  $w_i$  to the experimental drag of the cavity which produced the largest drag. These two sets of data indicate that a reasonable upper limit on the shear layer deflection is  $\eta_i \simeq 0.09$  for the range of variables investigated. Note that in some cases (i.e.,  $M_\infty > 1$  in Fig. 11) the resulting drag is much larger than the measured drag. This implies that the maximum deflection may be a function of Mach number of cavity size.

#### 4. Conclusions

The problem of cavity drag is seen to be dominated by the effects of cavity resonance over a wide range of variables. This resonance, particularly for subsonic internal flow, can increase the drag as much as 250%. Although the frequency of the pressure oscillations may be predicted by available methods, no known method is available for predicting the occurrence of this phenomenon.

This investigation casts doubt on the currently available experimental data on cavity drag. In most cases, the investigators were either not looking for or not cognizant of possible resonant effects.

Since the available analytical models for cavity drag have been formulated for the nonresonant case, they are inadequate when cavity resonance occurs. These models are also seen to be questionable for compressible flow with boundary

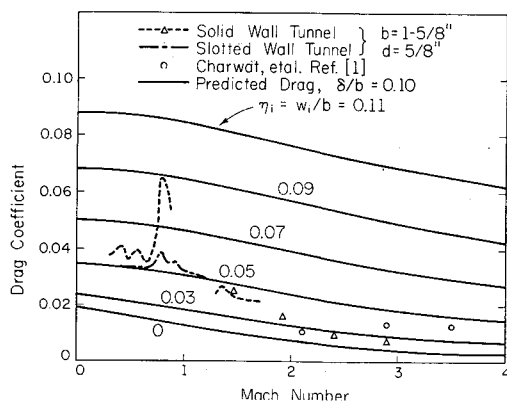


Fig. 11 Parametric description of effect of resonance on cavity drag with comparison to experimental data.

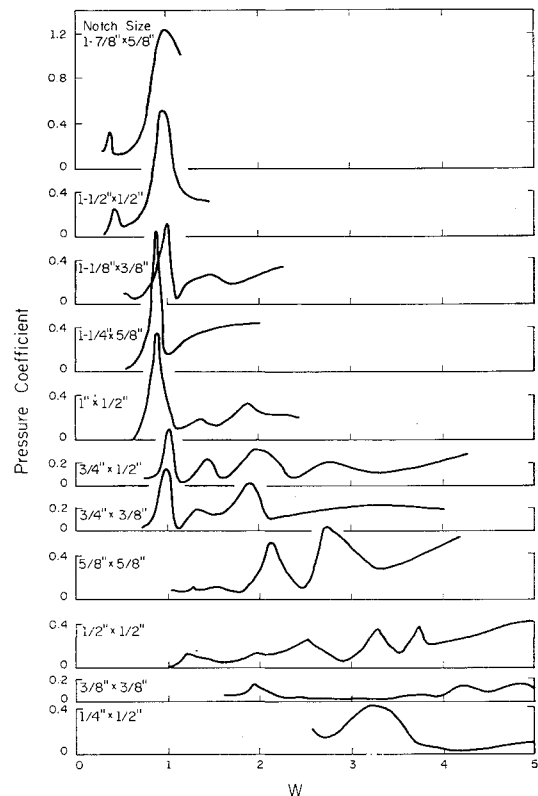


Fig. 12 Amplitude of pressure oscillations as a function of interaction parameter using frequency predicted by Eq. (1) with  $m - \beta = 0.75$  and  $\phi_e = 0.67$ .

layers. The new model presented here is believed to account for these effects and to define a lower bound on the cavity drag. The extension of the model to the case of resonant cavities is in qualitative agreement with the experimental data. This model, in conjunction with the experimental data presented here, should provide a reasonable guide for drag prediction until a more comprehensive model is developed.

#### Appendix: Effect of Wind-Tunnel Interference

When a resonating cavity is located on an interior surface of a flow system, e.g., inside a wind tunnel, reflections of the acoustic radiation can affect the strength of the resonance.<sup>20</sup> A simple model is proposed here which predicts both the magnitude and the occurrence of the interference.

The unsteady component of the pressure field is assumed to be composed of two sine waves of like frequency, but of different amplitude and phase. The reflected wave is assumed to decay inversely with the square root of the path length<sup>21</sup> from the amplitude of the main disturbance  $\Delta P_1$ . For a path length of twice the distance to the reflecting wall, the total number of wave lengths participating is

$$W = 2(h/b)M_\infty St / (1 - M_\infty^2)^{1/2} \quad (A1)$$

where  $h$  is the distance to the reflecting wall. The peak-to-peak amplitude of the combination of waves is then

$$\Delta P / \Delta P_1 = [1 + (2\alpha/W^{1/2}) \cos(2\pi W) + \alpha^2/W]^{1/2} \quad (A2)$$

where  $\alpha$  is the proportionality constant. For the data presented here  $\alpha \simeq 0.625$ .

As shown in Eq. (A2), pressure peaks occur near  $W = 1, 2, 3, \dots$ , as suggested by Spee,<sup>20</sup> while the valleys occur near  $W = \frac{1}{2}, \frac{3}{2}, \frac{5}{2}, \dots$ . Figure 12 shows the pressure data from the drag investigation plotted against the variable  $W$ . The effects of interference are clearly present for the larger notches ( $b/d = 2$  and  $3$ ). Peaks which do not occur at integer values

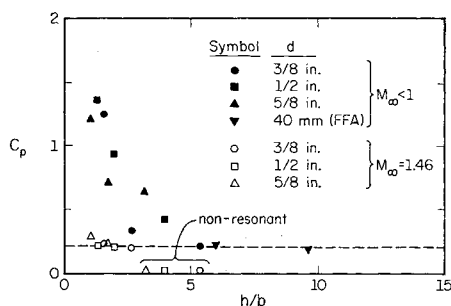


Fig. 13 Variation of amplitude of pressure oscillations at peaks as a function of wind-tunnel height.

of  $W$  are due to noninterference peaks and peaks caused by higher frequency modes. This analysis also shows that the effect of the reflected waves decreases with increasing Mach number and increasing path length (wind-tunnel height). Based on data currently available (see Fig. 13), this type of interference should be negligible when  $h/b > 5$ .

Note that this interaction phenomenon is a result of cavity resonance; it does not cause it. As shown by the frequency data in Fig. 7, the occurrence and frequency of resonance is not affected by reflected waves; only the strength is affected.

## References

- Charwat, F. F. et al., "An Investigation of Separated Flows; Part I: The Pressure Field," *Journal of the Aerospace Sciences*, Vol. 28, No. 6, 1961, pp. 457-470.
- Krishnamurty, K., "Acoustic Radiation from Two-dimensional Rectangular Cutouts in Aerodynamic Surfaces," TN-3487, 1955, NACA.
- Charwat, F. F. et al., "An Investigation of Separated Flows; Part II: Flow in the Cavity and Heat Transfer," *Journal of the Aerospace Sciences*, Vol. 28, No. 7, 1961, pp. 513-527.
- Rossiter, J. E., "Wind Tunnel Experiments on the Flow over Rectangular Cavities at Subsonic and Transonic Speeds," R & M 3438, (AD 805489), 1966, Aeronautical Research Council, Ministry of Supply, London.
- Golik, R. J., "On Dissipative Mechanisms within Separated Flow Regions (with Special Considerations to Energy Transfer across Turbulent Compressible  $Pr_t = 1$ , Mixing Regions)," Ph.D. thesis, 1962, Dept. of Mechanical and Industrial Engineering, Univ. of Illinois, Urbana, Ill.
- Haugen, R. L. and Dhanak, A. M., "Momentum Transfer in Turbulent Separated Flow Past a Rectangular Cavity," *Journal of Applied Mechanics*, Sept. 1966, pp. 641-646.
- Mehta, U. B. and Lavan, Z., "Flow in a Two-Dimensional Channel with a Rectangular Cavity," CR-1245, 1969, NASA.
- McGregor, O. W., "Aerodynamic Drag of Two-dimensional Rectangular Notches in Transonic and Supersonic Turbulent Flow (with Emphasis on the Effects of Self-induced Pressure Oscillations)," Ph.D. thesis, 1969, Dept. of Mechanical and Industrial Engineering, Univ. of Illinois, Urbana, Ill.
- "The FFA Aerodynamic Research and Test Facilities," Memo 33, 1964, The Aeronautical Research Institute of Sweden (FFA), Stockholm, Sweden.
- Howell, R. H., "Drag Forces of Two-dimensional V-shaped Notches in Transonic and Supersonic Turbulent Flow," Ph.D. thesis, 1968, Dept. of Mechanical and Industrial Engineering, Univ. of Illinois, Urbana, Ill.; also, CR-1132, 1968, NASA.
- Spalding, D. B. and Chi, S. W., "The Drag of a Compressible Turbulent Boundary Layer on a Smooth Flat Plate with and without Heat Transfer," *Journal of Fluid Mechanics*, Vol. 18, 1964, pp. 117-143.
- White, R. A. and McGregor, O. W., "Dynamics of Resonant Two-dimensional Cavities in Aerodynamic Surfaces at Transonic and Supersonic Mach Numbers," *Developments in Mechanics*, Vol. 4, *Proceedings of the Tenth Midwestern Mechanics Conference*, Colorado State Univ., Ft. Collins, Col., edited by J. E. Cernak and J. R. Goodman, 1967, pp. 1029-1046.
- Nyborg, W. L., "Self-maintained Oscillations of the Jet in a Jet-Edge System," *Journal of the Acoustical Society of America*, Vol. 26, No. 2, March 1954, pp. 174-182.
- Plumbee, H. E., Gibson, J. S., and Lassiter, L. W., "A Theoretical and Experimental Investigation of the Acoustical Response of Cavities in an Aerodynamic Flow," TR-61-75, (AD 277803), March 1962, Wright Air Development Div.
- Brown, G. B., "The Vortex Motion Causing Edge Tones," *Proceedings of the Physical Society*, Vol. 49, 1937, pp. 508-521.
- Korst, H. H. and Chow, W. L., "Non-isothermal Turbulent ( $Pr_t = 1$ ) Jet Mixing between Two Compressible Streams at Constant Pressure," CR-419, 1966, NASA.
- McGregor, O. W., "An Approximate Analysis of the Development of the Turbulent Shear Layer between Two Streams," unpublished.
- Abramovich, G. N., *The Theory of Turbulent Jets*, M. I. T. Press, Cambridge, Mass., 1963, pp. 56, 193.
- Maydew, R. C. and Reed, J. F., "Turbulent Mixing of Compressible Jets," *AIAA Journal*, Vol. 1, No. 6, 1963, pp. 1443-1444.
- Spee, B. M., "Wind Tunnel Experiments on Unsteady Cavity Flow at High Subsonic Speeds," *Proceedings of a Specialists Meeting: AGARD Conference Proceedings*, No. 4, 1966, Rhode-Saint-Genese, Brussels, Belgium.
- Morse, P. M., *Vibration and Sound*, McGraw-Hill, New York, 1948, p. 298.